

Dynamical bi-stability of single-molecule junctions: A combined experimental/theoretical study of PTCDA on Ag(111)

Thomas Brumme,^{*,†} Olga Neucheva,^{‡,¶} Cormac Toher,[†] Rafael Gutiérrez,[†]
Andreas Greuling,[§] Marcin Kaczmarek,[§] Michael Rohlfing,[§] Stefan Tautz,[‡] and
Gianaurelio Cuniberti[†]

*Institute for Materials Science and Max Bergmann Center of Biomaterials, Dresden University of
Technology, 01062 Dresden, Germany,*

*Institute for Bio- and Nanosystems-3 and JARA-Fundamental of Future Information Technology,
Forschungszentrum Jülich GmbH, 52425 Jülich, Germany,*

*Institute of Materials Research and Engineering, 3 Research Link, Singapore 117602, Republic of
Singapore, and*

Fachbereich Physik, Universität Osnabrück, 49069 Osnabrück, Germany

E-mail: thomas.brumme@nano.tu-dresden.de

Abstract

The dynamics of a PTCDA-Ag(111) molecular junction has been investigated experimentally and theoretically. Switching between two conductance states was observed by low-temperature scanning tunneling microscopy, and was dependent on the tip-substrate distance

*To whom correspondence should be addressed

[†]TU Dresden

[‡]Forschungszentrum Jülich

[¶]Singapore

[§]Universität Osnabrück

and the applied bias, but was less sensitive to the bias polarity. Using a minimal model Hamiltonian approach combined with density-functional calculations, the switching was shown to be related to the scattering of electrons tunneling through the junction, which progressively excite the relevant chemical bond. Depending on the direction in which the molecule switches, different molecular orbitals are shown to dominate the transport and thus the vibrational heating process. This in turn can dramatically affect the behavior of the switching rate, demonstrating the importance of modelling the DOS realistically.

The scanning tunnelling microscope (STM) is a valuable and versatile tool for the study and manipulation of nanoscale structures.^{1,2} In scanning mode, it can be used to image surfaces with atomic resolution, and to probe the electronic density of states at a range of energy values. Alternatively, it can be brought into contact with surface features to form junctions and measure transport properties. Nanostructures and devices can be manipulated and fabricated using an STM, with the possibility to pick up and deposit atoms and molecules using the tip.³⁻⁵ One of the most fascinating aspects related to the tip-molecule interaction is the telegraph noise observed in the conductance in certain circumstances, which is believed to be due to the repeated switching of single atoms or functional groups between different stable configurations.⁶⁻⁹ Several physical mechanisms have been proposed to explain this phenomenon: thermal activation, vibrational heating (for intermediate biases)¹⁰⁻¹⁴ and transition through an electronic excited state with no conformational bistability (for high biases).¹⁵ If the masses involved are not too large (i.e. for a single atom), quantum tunneling is also possible.¹⁶

In this Letter, we will present a systematic study on this switching behavior in the specific system of perylene-3,4,9,10-tetracarboxylic-dianhydride (PTCDA) on Ag(111), using both experimental and theoretical methods. With results from density-functional (DFT) calculations and by extending a microscopic model developed in Ref. 14 to describe the coupling of an adsorbate energy level to the adsorbate vibrational excitations, a good agreement with the experimentally measured switching rates can be achieved.

PTCDA deposited on Ag(111) forms a highly ordered metal-organic interface, the electronic

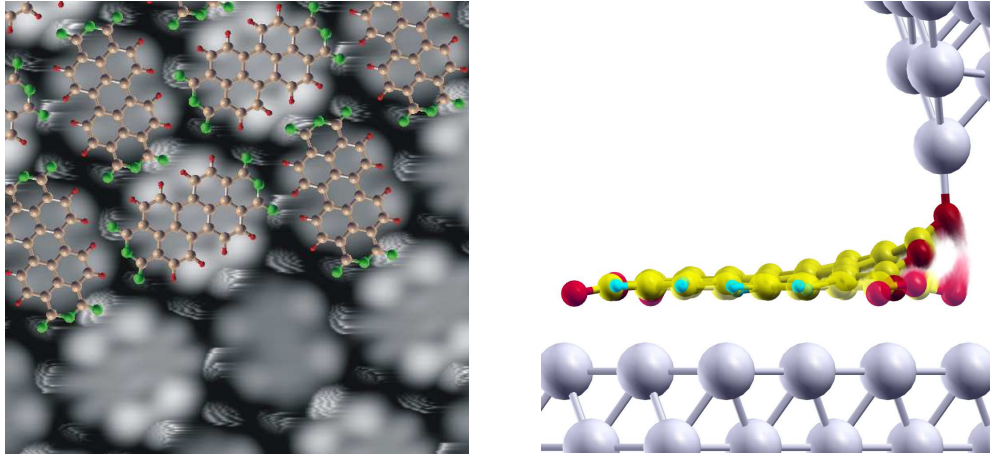


Figure 1: (color online) Left: Constant current STM image of a PTCDA layer measured with a functionalized tip at low tip height. The switching motion of the oxygen atoms is easily discernible at the corners of the PTCDA molecule. Bias: -4 mV, Current: 10 nA, monolayer surface: 5×5 nm². Right: Schematic picture illustrating the switching process of the carboxylic atom between the surface and the tip apex atom. The coordinates were taken from the DFT calculations described in Ref. 22.

and geometric structure of which has been well-characterized using a variety of both experimental and theoretical techniques.^{17–19} The PTCDA molecules form long-range ordered commensurate monolayers on the Ag(111) substrate with two flat-lying chemisorbed molecules per unit cell in a herringbone arrangement (see Fig. 1 and Ref. 17). Once the monolayer is formed the intermolecular interactions prevent the molecules from diffusing over the surface thus making the system suitable for STM experiments. The chemisorption results in the former lowest unoccupied molecular orbital (LUMO) of the isolated molecule being shifted below the Fermi level of the silver surface, so that there is charge transfer from the substrate to the molecule thus producing a net negative charge on the molecule. In previous experiments,²⁰ we have found that it is possible to form a chemical bond between the carboxylic oxygen atoms and the STM tip, and the formation of this molecular junction has been discussed in Ref. 21. Once the molecular junction has been formed with the tip there are two possible ways for the molecule to behave under the tip retraction: either it is peeled off from the surface completely or it falls back. In the course of these experiments, we have further observed that, under certain conditions, the current fluctuates in time between a high- and a low-conductance state. These fluctuations can be explained by the switching of the molecule

in and out of contact with the tip (see Fig. 1). This switching processes of the molecule can also be seen in the topographic images taken with the tip very close to the surface (cp. Fig. 1).

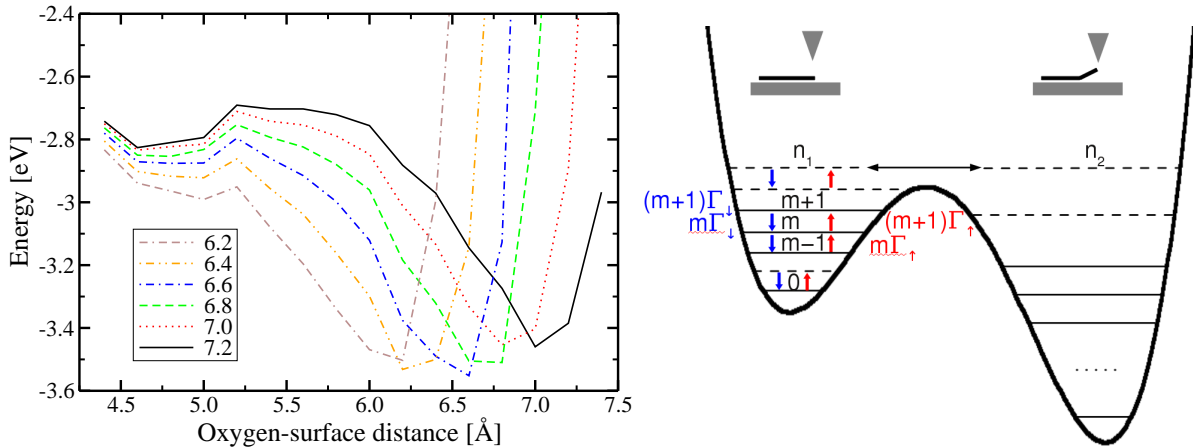


Figure 2: (color online) Left: Double well potentials for different tip–substrate separations calculated with DFT for a single PTCDA molecule.²² Right: Declaration of the model parameters. $\Gamma_{\downarrow/\uparrow}$ denote the relaxation and excitation rate of a molecular vibration due to scattering of tunneling electrons and n_1/n_2 denote the critical number of vibrations which have to be excited to induce the switching.

The primary factors determining which type of behavior is observed are the surrounding molecular environment and the applied bias. The intermolecular interactions play an important role for the molecular mobility. The isolated PTCDA molecules on the Ag(111) surface are known to diffuse over the substrate even at low temperatures.¹⁷ At low biases, the isolated molecule is relatively unstable and can be easily peeled off the surface during the cleaving process and remains attached to the tip. This behavior agrees with DFT calculations which show that the oxygen atom prefers to be attached to the tip when it is within 6Å of the surface²² (cp. Fig. 2). In contrast, a molecule residing inside the compact layer is very difficult to remove from the surface, due to strong intermolecular interactions via hydrogen bonds. As a result, the tip–molecule bond breaks during the tip retraction leading to the molecule remaining at the same position in the layer. As for the molecules at the edge of the monolayer, they display a behavior which is intermediate to these two possibilities. The carboxylic oxygen atoms which are free from neighboring molecules can react more easily with the STM tip, thus producing a higher switching rate in comparison with

the molecules residing inside the compact layer. However, the hydrogen bonding to the neighboring molecules prevents them from being removed from the surface. Thus, in the experiments, the “edge” molecules were chosen for the rigorous quantitative analysis of the switching process, which was the primary objective of this work.

The experiments have been performed with a low temperature scanning tunneling microscope (7K) in an ultrahigh vacuum with a base pressure under 10^{-10} mbar. The Ag(111) surface has been prepared by repeated sputtering/annealing cycles: sputtering a single crystalline metal surface using incident beam of Ar ions (ion beam energy 0.8keV) at room temperature followed by subsequent annealing at temperatures of about 850K. Control of the surface quality has been done in situ with low-energy electron diffraction (LEED) optics. The PTCDA molecules have been evaporated from a Knudsen cell (which is at 580K) onto the surface which is kept at room temperature. An electrochemically etched tungsten wire has been used for the STM tip, which has been cleaned in situ by annealing. The final atomic sharpening has been done by indentation of the tip into the clean metal substrate and/or by application of voltage pulses. The tip quality has been checked by measuring the surface state of Ag(111). The PTCDA material (commercial purity 99%) has been purified by resublimation and outgassing in ultra high vacuum for 100 hours. The first step of the analysis of the switching process is to count the number of switching events for the carboxylic oxygen between the silver surface and the STM tip. In order to perform the analysis of the switching process the tip was stabilized at a height above the carboxylic oxygen atom such that a current of 0.1nA was obtained at $V=-340$ mV. This tip height is greater than the distance region where repeated switching can be observed. Then the feedback loop was switched off and a voltage applied to the sample. The time spectra were recorded for different bias voltages and tip heights. The time dependent current $I(t)$ is shown in Fig. 3 for the applied bias voltage of 95mV and with the tip positioned at 7.3\AA above the substrate (see supplementary information for details on tip height estimation). The telegraph noise like behavior of the current is evident for the two conductance states of the molecular junction. The low current (low conductance) state corresponds to the tunneling regime in which all four carboxylic oxygen atoms are chemically bound to the surface,

whereas the high current (high conductance) state corresponds to the situation where one of the carboxylic oxygen atoms forms a chemical bond with the tip, thus forming a molecular junction between the tip and the substrate.

The switching map obtained from the STM measurements as a function of the bias voltage which is applied to the sample, as well as the tip height is shown in Fig. 3. It should be noted that the switching process takes place upon both tip approach and retraction (the case of retraction is not shown in the figure). The applied bias influences the number of switches as well as the tip height at which they start and end. For negative bias, the repeated switching region can be reached at greater tip heights than for positive bias. This is probably due to the fact that the PTCDA molecule is negatively charged with a large charge density on the carboxylic oxygens.²³ Therefore, applying a negative bias to the substrate leads to a repulsive electrostatic force between the net negative charge of the molecule and the surface, which in turn leads to an increase of the tip height where the switching process occurs. In contrast, at positive bias the substrate and the molecule attract each other so that smaller tip–surface distances are required to initiate the switching process.

From the $I(t)$ curve one can see that for the chosen bias and tip height, conformations where the oxygen atom is bound to the tip are preferred. The residence time analysis (Fig. 3) shows a difference of more than one order of magnitude in the residence time values for the high and low conductance states. The single exponential behavior of the curves indicate a two state Markovian switching process where the residence time probability $P_{0,1}$ is given by the expression $P_{0,1}(t) = R_{0,1} \exp(-R_{0,1}t)$. Here, $R_{0,1}$ is the transfer rate between the two conductance states. By performing a transfer rate analysis for different bias voltages one can determine the transfer rates as a function of bias for every measured distance. The rates for typical tip-substrate separations are displayed in Fig. 4.

To gain insight into the observed current switching, we first focus on the nature of the coupling between PTCDA and the surface, and then provide a link to the experimental data by applying model calculations. The mechanisms of the chemical bonding of PTCDA to Ag(111) includes hybridization of the molecular orbitals with the surface states, charge transfer between the surface

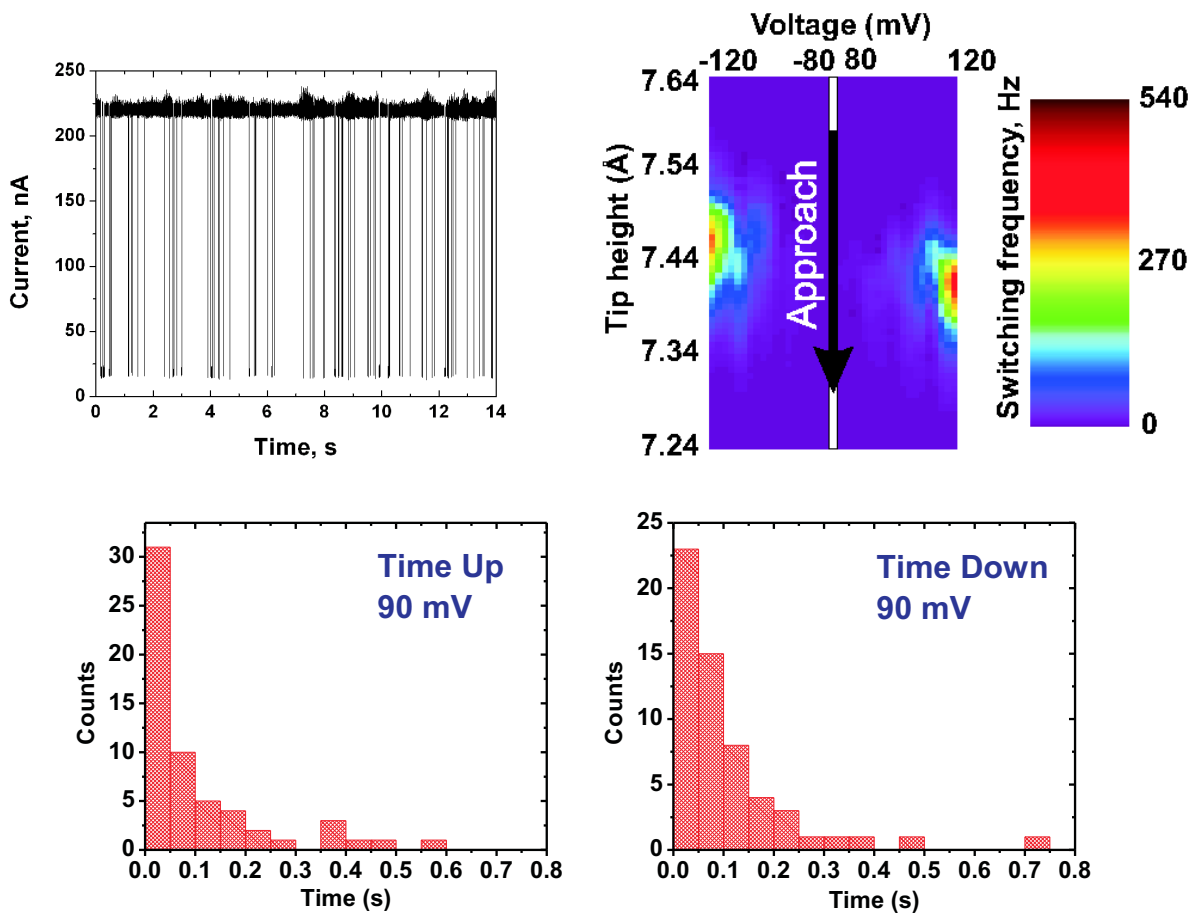


Figure 3: (color online) Switching of a single PTCDA molecule by tunneling current. Upper left: The time spectrum of a current measured at 95mV with a tip height of 7.6Å above the substrate reveals the “telegraph noise” behavior. Upper right: The switching map of the STM junction as a function of bias voltage and tip height. The initial spectra were measured at constant bias during tip approach. The bias range from -150mV to 150mV was covered with a step of 5mV. Lower: the first order exponential decay distribution of the residence times at low and high conductance states.

and the molecule, local bonds of the carboxylic oxygen and an extended bond of the molecular π -system to the surface.²⁰ However, as already mentioned above, the situation changes if a bias is applied. Assuming that the two meta-stable positions can be well-represented by a (not necessarily symmetric) double-well potential, the transfer of an adsorbate between the two minima can involve a variety of physical processes such as (i) thermal activation, (ii) quantum tunneling, (iii) a transition through an electronic excited state with no conformational bistability, or (iv) vibrational heating. The processes (i) and (ii) are of minor interest in this work, since the experiments are performed at very low temperatures (7K) and the barrier height is larger than 100meV,²² which excludes the thermal activation; and process (ii) seems very improbable, due to the relatively large mass of the part of the molecule involved in the switching process. Even if one assumes that only the carboxylic oxygen switches the corresponding transfer rate would be negligibly small. For process (iii), which involves an excited state of the molecule, the residence time of the tunneling electrons has to be sufficiently large to induce this excitation. However, due to the molecule being chemisorbed on the Ag(111) surface, the residence time becomes quite small, so that process (iii) also seems unlikely in this case. Thus, we suggest that the microscopic mechanism leading to switching is related to vibrational heating, where the transition (bond breaking) is induced by progressive vibrational excitation of the relevant chemical bond (*e.g.*, the oxygen-substrate bond). The transition rate is then mainly determined by the competition between energy gain from the tunneling charges and energy losses due to electron-hole pair generation and/or coupling to the substrate phonon continuum. In this work, we will neglect the coupling to the substrate phonon continuum, since the anharmonic coupling is, in general, very small at low temperatures.

We have applied a minimal model approach based on that used in Ref. 14 to describe the vibrational heating. The Hamiltonian has the following form:

$$\begin{aligned}
H_e = & \sum_s \varepsilon_s c_s^\dagger c_s + \sum_t \varepsilon_t c_t^\dagger c_t + \varepsilon_m c_m^\dagger c_m \\
& + \sum_s \left(T_{sm} c_s^\dagger c_m + H.c. \right) + \sum_t \left(T_{tm} c_t^\dagger c_m + H.c. \right) .
\end{aligned} \tag{1}$$

It describes the tunneling of electrons between the STM tip and the surface via an adsorbate level (in this case, the adsorbate being the PTCDA molecule). Here s , t and m label one-electron states $|s\rangle$, $|t\rangle$ and $|m\rangle$ of the surface, the tip and the molecule, respectively, with the corresponding energies ε_s , ε_t and ε_m . The hopping between the surface and the tip via the molecular level is described by the last two terms in Eq. (1).

The coupling between the vibrational motion of the molecule and the electron propagating through it is modeled by assuming that ε_m is a linear function of the vibrational coordinate q , $\varepsilon_m(q)$. Hence, the total Hamiltonian for the electrons and the molecular vibration can be written as:¹⁴

$$H = H_e + \hbar\omega b^\dagger b + \sqrt{\frac{\hbar}{2M\omega}} (b^\dagger + b) (\varepsilon'_m c_m^\dagger c_m - \varepsilon'_{m0} n_{m00}) \quad . \quad (2)$$

Here, ω is the frequency of the molecular vibration with the normal coordinate $q = \sqrt{\frac{\hbar}{(2M\omega)}} (b^\dagger + b)$ and mass M , and $\varepsilon'_m = \partial\varepsilon_m/\partial q$ at $q = 0$. The counterterm $-\varepsilon'_{m0} n_{m00}$, with $n_{m00} = \langle c_m^\dagger c_m \rangle_{V=0}$ being the average occupation of the molecular level at $V = 0$ and $q = 0$, and with $\varepsilon'_{m0} = \varepsilon'_m$ at $V = 0$, ensures that the average force on the oscillator is zero for $V = 0$ at $q = 0$.

Since the effect of the electron-vibration interaction (the last term of Eq. (2), H_{e-v}) on the adsorbate vibration is in general weak, it can be treated by first-order perturbation theory. The assumed linearity in the charge-vibron coupling simplifies the problem since only the excitation and relaxation rates, Γ_\uparrow and Γ_\downarrow , between the vibrational ground state and the first excited state are required (cp. Fig. 2). In first-order perturbation theory these transition rates are given by Fermi's Golden Rule:

$$\begin{aligned} \Gamma_\downarrow &= 2\frac{2\pi}{\hbar} \sum_{j,l} |\langle j, 0 | H_{e-v} | l, 1 \rangle|^2 f_l (1 - f_j) \delta(\varepsilon_j - \varepsilon_l - \hbar\omega), \\ \Gamma_\uparrow &= 2\frac{2\pi}{\hbar} \sum_{j,l} |\langle j, 1 | H_{e-v} | l, 0 \rangle|^2 f_l (1 - f_j) \delta(\varepsilon_j - \varepsilon_l + \hbar\omega), \end{aligned} \quad (3)$$

where 0 and 1 are the vibrational ground state and the first excited state, respectively, and j and l denote any of the stationary one-electron states of the tip or the substrate with corresponding Fermi-

Dirac distributions $f_{j,l} = 1/\{1 + \exp[(\varepsilon - \varepsilon_{l,j})/(k_B T)]\}$. These rates describe the vibrational decay into substrate or tip continua due to electron-hole pair excitations. Since the initial and the final states can be either a tip or a substrate state, these rates can be decomposed into four different terms: $\Gamma_{\uparrow,\downarrow}^{ss}$, $\Gamma_{\uparrow,\downarrow}^{tt}$, $\Gamma_{\uparrow,\downarrow}^{st}$ and $\Gamma_{\uparrow,\downarrow}^{ts}$, which sum up to give $\Gamma_{\uparrow,\downarrow}$. Here, the first (second) superscript denotes whether the final (initial) state belongs to the surface or the tip. In contrast to Ref. 14, we will not assume that the adsorbate local DOS is constant over the relevant energy range, but rather we model it by a Lorentzian shape, $\rho_m(E) = \Delta/((E - \varepsilon_m)^2 + \Delta^2)$, where $\Delta = \Delta_s + \Delta_t$, with Δ_s and Δ_t describing the coupling between the molecular level and the substrate and tip electronic states, respectively. Using this function, the excitation and relaxation rates can be calculated analytically in the low temperature limit, *e.g.*:

$$f_{\pm}(\varepsilon) = \frac{\left((\varepsilon_m - \varepsilon_F)^2 + \Delta^2\right)^2}{\Delta \hbar^2 \omega^2 (4\Delta^2 + \hbar^2 \omega^2)} \left(\hbar\omega \tan^{-1} \left[\frac{\varepsilon_m - \varepsilon_F + \varepsilon}{\Delta} \right] \pm \Delta \log \left[\Delta^2 + (\varepsilon_m - \varepsilon_F + \varepsilon)^2 \right] \right) \quad (4)$$

$$\Gamma_{\downarrow}^{st} = \sqrt{\gamma_{eh}^s \gamma_{eh}^t} \left(f_+(eV + \hbar\omega) + f_-(eV) - f_+(0) - f_-(-\hbar\omega) \right)$$

$$\Gamma_{\uparrow}^{st} = \sqrt{\gamma_{eh}^s \gamma_{eh}^t} \left(f_+(eV) + f_-(eV - \hbar\omega) - f_+(\hbar\omega) - f_-(0) \right) .$$

The constants $\gamma_{eh}^{s,t}$ describe the level broadening due to the coupling of tunneling electrons of the tip (*t*) and the surface (*s*) with the vibrations of the molecule. In contrast to all other parameters, *e.g.* the broadening Δ or the energy ε_m , it is in general difficult to determine them from experiment or *ab-initio* calculations. Fortunately, these are only prefactors which change the absolute height of the transition rates and thus can be easily fit to the experiments. We refer the interested reader to the supplementary material for further details and a comprehensive description of the calculation. To describe the transfer between the two possible meta-stable states a truncated harmonic oscillator model, as described in Ref. 14, is adopted. The escape rate R can be expressed as a product of the transition into level n (see Fig. 2) and an effective Boltzmann factor describing the probability to

arrive at the sub-critical level $n - 1$ where the transition takes place:¹⁴

$$R \simeq n\Gamma_{\uparrow} \left(\frac{\Gamma_{\uparrow}}{\Gamma_{\downarrow}} \right)^{n-1} . \quad (5)$$

Since the adsorbate local DOS is not assumed to be constant over the relevant energy range, the above expression in general does not yield a simple power law dependence on the applied bias as in Ref. 14 ($R \propto V_{bias}^n$). Only if the molecular level is far apart from the Fermi energy (nearly constant DOS at E_F), can this simple scaling law be recovered.

Using Eqs. (4), (11), (14) and (15) we are now able to fit the transfer rate in Eq. (5) to the experimental results. DFT calculations²² were used to determine reasonable starting values and boundaries for the fitting parameters, such as the position of the molecular level ϵ_m and the broadening Δ . The levels on either side of the Fermi energy are, as would be anticipated, the most important channels for the tunneling electrons. The fitting procedure showed that, if the molecule is attached to the STM tip, the charge primarily tunnels through the level below the Fermi energy, while the level above is more important when the molecule is flat on the surface. Furthermore, the vibrational energy $\hbar\omega$ (*i.e.* the size of the steps on the “vibrational ladder”) was determined from the curvature of the calculated potential energy surfaces, shown in Fig. 2 and Ref. 22. They range from 19meV to 19.5meV for the shallower well where the molecule is switched down to the surface (lower vibrational mode), and from 40.6meV to 41meV for the deeper well where the molecule is switched up to the tip (higher vibrational mode), depending on the tip–surface distance. Theoretical calculations show that near the lower (higher) vibrational mode several out-of-plane (in-plane) vibrations of the carboxylic oxygen can be found.²⁴ To obtain a series of model-parameters that can be compared with the DFT data and the experiment, the higher vibrational mode and the level below ϵ_F were used for PTCDA switching from tip to surface, whereas for the reverse process the lower vibrational mode and the level above the Fermi energy were chosen. The exact values for the vibrational energies obtained from the slope of the potential energy surface calculated using DFT²² can be found in the supplementary information (Tab. 2).

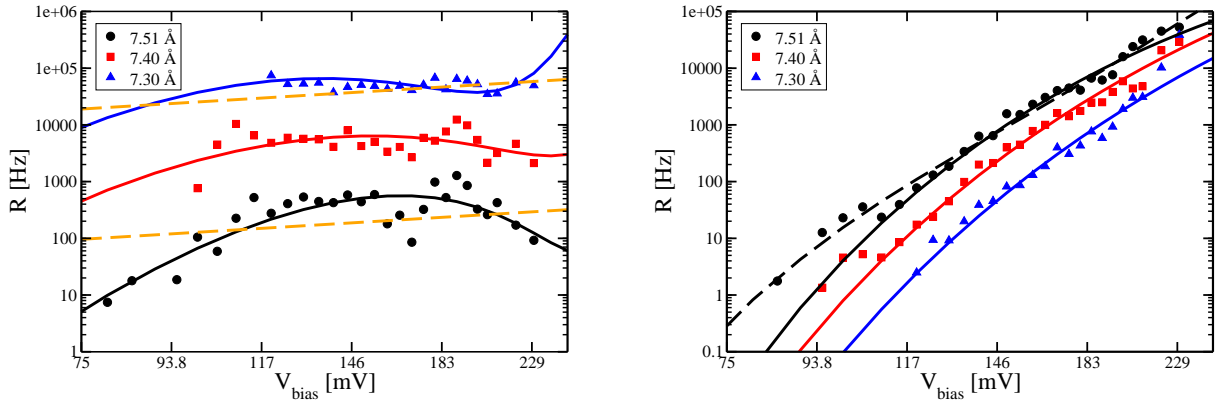


Figure 4: (color online) Log-Log-Plot of the transfer rate for PTCDA switching between an STM tip and a Ag(111) surface for different tip–surface separations. Measured transfer rate for switches from (left) tip to surface and (right) surface to tip are indicated by small symbols. Solid lines display the theoretical transfer rate, (left) dashed orange lines the model of Ref. 14, (right) dashed black line the theoretical transfer rate taking both levels near the Fermi energy into account.

Figure 4 shows the experimental results together with the theoretical model calculations for three tip–surface distances for the transfer rate of the PTCDA molecule between the tip and the silver surface. The rate at which the molecule switches from the tip to the surface increases monotonically with applied bias in the given voltage range, but the rate at which it switches from the surface to the tip appears to have a maximum around 120mV. The rate is dependent on the tip–surface distance, as can also be seen in the experimental data in Fig. 3. Finally, there also appear to be jumps in the switching rate around certain bias voltages, e.g. 110mV and 160mV. Each of these properties will be discussed and explained below.

The fitting parameters obtained for different tip-surface distances are shown in Tab. 1 and in Tab. 3 in the supplementary information. These values can be understood by considering the potential energy surfaces obtained from DFT calculations,²² where it was shown that it is energetically more favorable for a carboxylic oxygen atom in a single PTCDA molecule on an Ag(111) surface to be attached to the tip than to the surface. Therefore, the potential energy surface is a highly asymmetric double well with a shallow well at the surface and a deep one at the tip, with the asymmetry increasing as the tip–surface distance is reduced, see Fig. 2. The potential well at the

Table 1: Model-parameters for the switching of the PTCDA between the tip to the surface obtained by fitting R to the experiments. The subscript “1” and “2” indicate switching from STM tip to the surface or the reverse process, respectively. Parameters $\gamma_{eh,1}^{s/t}$ and $\gamma_{eh,2}^{s/t}$ are given in units of $[10^7 \text{ 1/s}]$ or $[10^5 \text{ 1/s}]$, respectively. Energies ϵ_m are given in meV .

Tip–surface distance	$\gamma_{eh,1}^s$	$\gamma_{eh,1}^t$	$\epsilon_{m,1}$	n_1
7.30 Å	8.30	0.95	−960	15
7.40 Å	9.96	1.39	−778	14
7.51 Å	9.85	3.20	−427	14

Tip–surface distance	$\gamma_{eh,2}^s$	$\gamma_{eh,2}^t$	$\epsilon_{m,2}$	n_2
7.30 Å	22.84	5.02	249	9
7.40 Å	1.41	0.70	296	10
7.51 Å	0.45	0.01	296	10

surface reduces to a saddle point for tip–surface distances of less than about 6.2Å. These changes in the shape of the double well potential correspond to a decreasing (increasing) barrier height for surface to tip (tip to surface) switches with decreasing tip–surface distance.

However, as can be seen in the values in the rightmost column of Tab. 1, this change in the potential does not seem to have a major effect on the number of vibrational levels, n . This is due to the fact that changing the tip–surface distance alters the strength of the bonds between the adsorbate level, tip, and surface, thus leading to small changes in the vibrational frequency which partially compensate for the change in barrier height (cp. Tab. 2). The depth of the potential well at the tip ($n_1 * \hbar\omega_1$) also agrees with those calculated within DFT, whereas the well of the surface in the model is slightly deeper than those derived from the *ab-initio* calculations (cp. Fig. 2). This is due to the fact, that the potentials were calculated for a single PTCDA molecule, whereas in the experiments the edge molecules were used. The hydrogen bonds to the neighboring molecules will, however, lead to a significant increase of the barrier height.

In fact, the change in the switching rate with tip–surface distance appears to be due to changes in the adsorbate DOS. The DFT calculations and experiments²² predict that, if the PTCDA is attached to the tip, the level ϵ_m moves towards ϵ_F with increasing tip–surface distance. This behavior can also be seen in the values obtained during the fitting procedure. The agreement between the-

ory and experiment can even be improved by taking both levels near the Fermi energy into account (dashed line in Fig. 4). This, however, renders the fitting procedure questionable because of the increased number of parameters. On the contrary, if the PTCDA molecule is attached to the surface, the level is fixed. However, in the minimal model adopted here, its location changes between 0.24eV and 0.29eV.

Figure 4 also shows that the behavior of the transfer rate for switching from the surface to the tip switches is qualitatively different than that for the tip to the surface. First there is a small increase and then saturation of the transfer rate at about 120mV, with large fluctuations. A reasonable description within the model of Gao *et al.*¹⁴ is very unlikely (dashed orange lines in Fig. 4), because a fit is only possible by assuming $n = 1$, which is in contrast to the calculated potential energy surfaces, see Fig. 2. However, we were able to fit our model to the measurements by using the narrow molecular level above the Fermi energy (which follows the chemical potential of the surface) which can be found in DFT calculations.^{20,22} The increase of the theoretical calculated transfer rate above 220meV is due to the sudden increase of the DOS if the narrow molecular level gets into the bias window. Unfortunately, this increase cannot be observed in the experiments because the molecule normally disintegrates at lower biases than this because of the high current density.

The parameters $\gamma_{eh,1/2}^{s/t}$ listed in Tab. 1 and Tab. 3 also agree qualitatively with what one would expect on the basis of physical intuition. The influence of the tip is about one order of magnitude smaller than that of the surface. The curvature of the fitted curves, which is in contrast to the linear dependence on V_{bias} in the simpler model of Gao *et al.*,¹⁴ is due to the molecular level being described by a Lorentzian shape, the center of which is situated below or above the Fermi energy.

Taking a closer look at the experimental results (Fig. 4), it appears that there are sudden decreases of the switching rate at certain bias voltages, *e.g.* near 0.11eV or 0.16eV. This behavior is also observed for negative bias polarities and in both cases, the bias at which a jump takes place as well as the bias separation between consecutive jumps turns out to be very similar. The appearance of these kinks –which might have been observed for other molecules⁸– could either be related to a

change of the potential energy surface induced by the applied bias voltage, which would increase or decrease the number of vibrations the electrons have to excite, or to a greater influence of rapid barrier recrossing, if the critical vibrational levels in the two truncated harmonic oscillators are in resonance. The influence of the bias voltage on the potential can be modeled by a mutual linear shift of the two potential wells representing the tip and the surface. However, this would only introduce sudden decreases for one polarity of the bias, whereas for the other polarity a steep increase would occur. Since the experimental results show decreases for both positive and negative bias, this behavior can not be explained by this effect alone. Thus, an enhanced influence of the rapid barrier recrossing, if the critical vibrational levels in the two truncated harmonic oscillators are in resonance, may play a major role. Developing methods which take this effect into account is one of the goals of ongoing research.

Switching between low- and high conductance states has been observed in a single molecule junction consisting of a PTCDA molecule on a silver (111) substrate and contacted by an STM tip. The rates for the transition between these two states can be sensitively tuned by varying the applied bias as well as the tip-molecule separation. A vibrational heating mechanism where molecular bonds are excited by tunneling charges has been proposed to interpret the experimental results. Switching rates were calculated within a minimal model Hamiltonian approach describing the interaction between tunneling electrons and local molecular vibrations. The experimental results could be fitted over a broad voltage range for the cases where the PTCDA molecule switches both from the surface to the tip and from the tip to the surface. This is an improvement to the frequently used model which assumes the DOS to be constant and which can only fit switching from the tip to the surface, and demonstrates that it is crucial to take the non-constant behavior of the molecular DOS into account.

Acknowledgement

This work has been supported by the German Priority Program “Quantum transport at the molecular scale (SPP1243)”. The authors acknowledge the Center for Information Services and High

Performance Computing (ZIH) at the Dresden University of Technology for computational resources.

Supporting Information Available

Tip height calibration– The values for the tip height were calculated in the following way: it is known that the acquisition time for 1 point is $8\mu\text{s}$. The initial and final tip heights are set by the STM program. Knowing the difference between these heights and the time the tip has to travel it, one can calculate the tip velocity, which gives the possibility to determine the tip height as a function of time at every point with a simple equation:

$$z(t) = z_{start} + \frac{z_{end} - z_{start}}{t_{spectrum}} \times t, \quad (6)$$

where t can be defined as $t = i/125000$ (i –number of point in the raw spectrum), z is the relative tip height defined by the STM program, and $t_{spectrum}$ is the spectrum duration. In order to determine the absolute value of this coordinate, two types of additional experiments have been performed. The first one is contacting the bare silver surface (described in the supplementary information of Ref. 21). In this method the STM-tip touches the surface, which corresponds an the increase in the conductance to a value larger than the quantum of conductance. The second method for absolute tip height estimation is based on the measurement of a current above the molecule as a function of tip height. The tunnelling current decays exponentially with increasing distance between the tip and the surface:

$$I = I_0 e^{-2kz} \quad (7)$$

where k is a decay constant and related to the local barrier height Φ by:

$$k = \frac{\sqrt{2m\Phi}}{\hbar}. \quad (8)$$

However, the decay constant cannot be derived from the formula due to the unknown local barrier

height (apparent work function), which is:

$$\Phi = \frac{\Phi_{tip} + \Phi_{surface}}{2} \quad . \quad (9)$$

The work functions of Ag(111) and PTCDA/Ag(111) interface are known to be 4.74eV²⁵ and 4.75eV,²⁶ respectively. The work function of the tip, Φ_{tip} , is difficult to define due to the combination of two materials (tungsten covered by silver for the tip and PTCDA and silver for a surface) and the uncertain shape of the tip. To define the absolute tip height above the surface the decay constant values should be calculated. This should be done within the low bias region in order to exclude the influence of the bias on the electronic structure of the junction. Current was measured as a function of the distance above the carboxylic oxygen of the molecule. The current at 4mV is plotted in Fig. 5(a). Fitting the current curve with the exponential growth gives a value of 0.98 for the decay constant. The current as a function of distance can also be calculated theoretically. The current was calculated with the help of the non-equilibrium Green's function formalism.²⁷ The value for a decay constant for 4mV is 1.1 which is comparable with that obtained experimentally. From Eq. (7) and theoretical results the prefactor I_0 is equal to 0.0013A. Using this value for fitting experimental data, the formula for absolute height calculation can be derived:

$$z_{tipheight} = 10.8 - z_{STM\ program} \quad . \quad (10)$$

The comparison of the conductance of the junction obtained experimentally and theoretically is shown in Fig. 5(b). Both methods (tip crash²¹ and current measurements) give similar values for the tip heights where the switches occur. The disagreement between them is about 0.2Å. Although good agreement of the results obtained by different rescaling methods is obtained, the error of the distance estimation is relatively large ($\pm 0.5\text{Å}$) due to several factors: tip state, STM program set-point reproducibility, etc. However, since the tip does not change during one series of experiments, the influence of the tip state can be excluded leading to smaller errors within one series of the measurements.

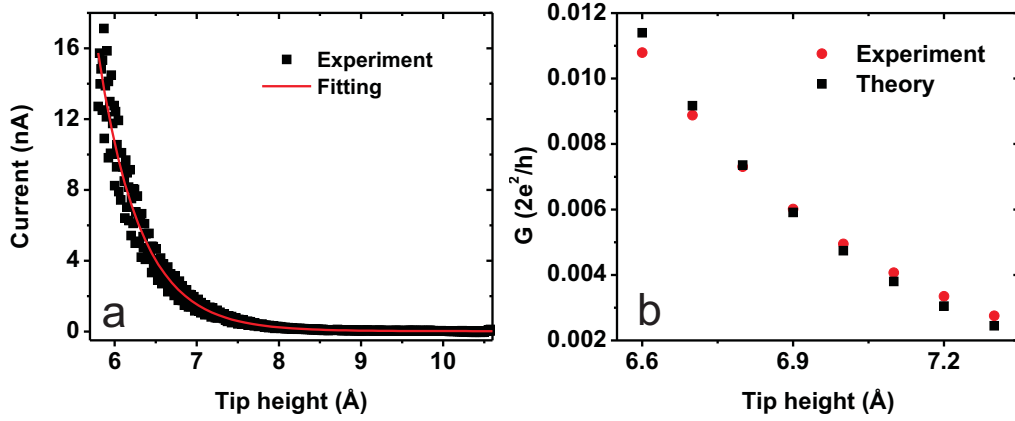


Figure 5: (color online) (a) Current spectrum of the STM junction as a function of tip height (black points – measured data, red curve – exponential decay fitting) measured during approach to a carboxylic oxygen. (b) Conductance spectra of the STM junction as a function of tip height (red points – experimental results based on (a), black points – calculated values) measured/computed for the approach of a tip to a carboxylic oxygen. The tip heights are scaled according to the performed fitting procedure (see text for details).

Calculation of the transition rates– In the following we want to sketch the derivation of the transition and relaxation rates given in Eq. (4). The terms $\Gamma_{\uparrow,\downarrow}^{ss}$ and $\Gamma_{\uparrow,\downarrow}^{tt}$ are all similar, and its sufficient to calculate explicitly only the term Γ_{\downarrow}^{ss} . Inserting Eq. (2) into Eq. (3) together with the

expression for the molecular DOS gives

$$\begin{aligned}
\Gamma_{\downarrow}^{ss} &= 2 \frac{\pi (\epsilon'_m)^2}{M \omega} \sum_{\alpha', \alpha} |\langle \alpha' | m \rangle \langle m | \alpha \rangle|^2 [1 - f_s(\epsilon_{\alpha'})] f_s(\epsilon_{\alpha}) \delta(\epsilon_{\alpha'} - \epsilon_{\alpha} - \hbar\omega) \\
&= 2 \frac{\pi (\epsilon'_m)^2}{M \omega} \int d\epsilon \rho_m^s(\epsilon) \rho_m^s(\epsilon + \hbar\omega) [1 - f_s(\epsilon + \hbar\omega)] f_s(\epsilon) \\
&= 2 \frac{\Delta_s^2 (\epsilon'_m)^2}{M \omega \pi} \int d\epsilon \frac{1}{[\epsilon - \epsilon_m]^2 + \Delta^2} \frac{1}{[\epsilon + \hbar\omega - \epsilon_m]^2 + \Delta^2} [1 - f_s(\epsilon + \hbar\omega)] f_s(\epsilon) \\
&\approx 2 \frac{\Delta_s^2 (\epsilon'_m)^2}{M \omega \pi} \int d\epsilon \frac{1}{[\epsilon - \epsilon_m]^2 + \Delta^2} \frac{1}{[\epsilon + \hbar\omega - \epsilon_m]^2 + \Delta^2} \\
&\quad \times [1 - \Theta(\epsilon_{F_s} - \hbar\omega - \epsilon)] \Theta(\epsilon_{F_s} - \epsilon) \\
&= 2 \frac{\Delta_s^2 (\epsilon'_m)^2}{M \omega \pi} \int_{\epsilon_{F_s} - \hbar\omega}^{\epsilon_{F_s}} d\epsilon \frac{1}{[\epsilon - \epsilon_m]^2 + \Delta^2} \frac{1}{[\epsilon + \hbar\omega - \epsilon_m]^2 + \Delta^2} \\
&= \frac{2 \Delta_s^2 (\epsilon'_m)^2}{M \pi \Delta \hbar \omega^2 (4 \Delta^2 + \hbar^2 \omega^2)} \left\{ \hbar \omega \left(\tan^{-1} \left[\frac{\epsilon_m - \epsilon_{F_s} + \hbar\omega}{\Delta} \right] \right. \right. \\
&\quad \left. \left. - \tan^{-1} \left[\frac{\epsilon_m - \epsilon_{F_s} - \hbar\omega}{\Delta} \right] \right) + \Delta \left(\log \left[\Delta^2 + (\epsilon_m - \epsilon_{F_s} + \hbar\omega)^2 \right] \right. \right. \\
&\quad \left. \left. + \log \left[\Delta^2 + (\epsilon_m - \epsilon_{F_s} - \hbar\omega)^2 \right] - 2 \log \left[\Delta^2 + (\epsilon_m - \epsilon_{F_s})^2 \right] \right) \right\} \quad (11)
\end{aligned}$$

In the first step the sum over states has been replaced with an integral over ϵ by introducing $\rho_m^s(\epsilon)$. In the second step the expression for the molecular DOS was used to rewrite the local density of states. Since the STM experiments are carried out at 7K one can approximate the Fermi function with the Heaviside step function in the next step. Thus, the limits of the integral can be changed from $+\infty$ and $-\infty$ to ϵ_{F_s} or $\epsilon_{F_s} - \hbar\omega$ respectively. With a new constant

$$\gamma_{eh}^{s,t} = \frac{2 \pi \hbar}{M} (\epsilon'_m)^2 (\rho_m^{s,t}(\epsilon_{F_{s,t}}))^2, \quad (12)$$

we finally get the expression in Eq. (4). The influence of an applied bias can be easily introduced by shifting the Fermi level of the surface $\epsilon_{F_s} = \epsilon_{F_{0s}} + eV$, where $\epsilon_{F_{0s}}$ is the Fermi level at $V = 0$ of the surface. Since we used the low temperature approximation in step 3 of Eq. (11) the excitation

rates $\Gamma_{\uparrow}^{ss,tt}$ become zero, because of the Pauli exclusion principle. The Pauli exclusion principle also simplifies the calculation of the remaining terms $\Gamma_{\uparrow,\downarrow}^{ts}$ and $\Gamma_{\uparrow,\downarrow}^{st}$, which describe the transition rates due to the inelastic scattering of tunneling electrons between surface and tip. Assuming $\varepsilon_{Ft} = \varepsilon_{Fs} := \varepsilon_F$, for negative applied bias the tunneling from surface to tip through the adsorbate level is prohibited. The excitation is forbidden because all states at the tip are occupied up to the energy ε_F , thus making it impossible for an electron from the surface with energy $\varepsilon_F - |eV| - \hbar\omega$ to tunnel to the tip. The probability of relaxing an adsorbate vibrations due to the inelastic scattering of tunneling electrons from the surface to the tip is negligible small, because the scattered electron would need several $\hbar\omega$ to gain enough energy. But this process can also be excluded, since the electron-vibration interaction on the adsorbate vibration is in general weak and we treat it by first-order perturbation theory. Thus, the transition rates can be written as,

$$\Gamma_{\uparrow}^{st} = \begin{cases} \frac{2\pi(\varepsilon'_m)^2}{M\omega} \int_{\varepsilon_F - |eV| + \hbar\omega}^{\varepsilon_F} d\varepsilon \rho_m^s(\varepsilon - \hbar\omega) \rho_m^t(\varepsilon) & \forall |eV| > \hbar\omega \\ 0 & \forall |eV| \leq \hbar\omega \end{cases} \quad (13)$$

$$\Gamma_{\uparrow}^{st} \stackrel{|eV| \geq \hbar\omega}{=} C^{st} \left\{ \begin{aligned} & \hbar\omega \left(\tan^{-1} \left[\frac{-\varepsilon_m + \varepsilon_F}{\Delta} \right] + \tan^{-1} \left[\frac{\varepsilon_m - \varepsilon_F + |eV|}{\Delta} \right] \right. \\ & \left. + \tan^{-1} \left[\frac{\varepsilon_m - \varepsilon_F - \hbar\omega + |eV|}{\Delta} \right] + \tan^{-1} \left[\frac{-\varepsilon_m + \varepsilon_F - \hbar\omega}{\Delta} \right] \right) \\ & + \Delta \left(\log \left[\Delta^2 + (\varepsilon_m - \varepsilon_F)^2 \right] + \log \left[\Delta^2 + (\varepsilon_m - \varepsilon_F + |eV|)^2 \right] \right. \\ & \left. - \log \left[\Delta^2 + (\varepsilon_m - \varepsilon_F - \hbar\omega + |eV|)^2 \right] - \log \left[\Delta^2 + (\varepsilon_m - \varepsilon_F + \hbar\omega)^2 \right] \right) \end{aligned} \right\}, \quad (14)$$

$$\begin{aligned}
\Gamma_{\downarrow}^{st} &= 2 \frac{\pi (\varepsilon'_m)^2}{M \omega} \int_{\varepsilon_F - |eV| - \hbar\omega}^{\varepsilon_F} d\varepsilon \rho_m^s(\varepsilon + \hbar\omega) \rho_m^t(\varepsilon) \\
&= C^{st} \left\{ \hbar\omega \left(\tan^{-1} \left[\frac{\varepsilon_m - \varepsilon_F + |eV|}{\Delta} \right] + \tan^{-1} \left[\frac{-\varepsilon_m + \varepsilon_F + \hbar\omega}{\Delta} \right] \right. \right. \\
&\quad \left. \left. + \tan^{-1} \left[\frac{\varepsilon_m - \varepsilon_F + \hbar\omega + |eV|}{\Delta} \right] + \tan^{-1} \left[\frac{-\varepsilon_m + \varepsilon_F}{\Delta} \right] \right) \right. \\
&\quad \left. + \Delta \left(\log [\Delta^2 + (\varepsilon_m - \varepsilon_F - \hbar\omega)^2] + \log [\Delta^2 + (\varepsilon_m - \varepsilon_F + \hbar\omega + |eV|)^2] \right. \right. \\
&\quad \left. \left. - \log [\Delta^2 + (\varepsilon_m - \varepsilon_F)^2] - \log [\Delta^2 + (\varepsilon_m - \varepsilon_F + |eV|)^2] \right) \right\} , \tag{15}
\end{aligned}$$

with

$$C^{st} = \sqrt{\gamma_{eh}^s \gamma_{eh}^t} \frac{\left((-\varepsilon_m + \varepsilon_F)^2 + \Delta^2 \right)^2}{\Delta \hbar^2 \omega^2 (4\Delta^2 + \hbar^2 \omega^2)} . \tag{16}$$

The $\gamma_{eh}^{s,t}$ are important parameters in our theory, as one can clearly see in the Eqs. (11), (14) and (15). In contrast to all other parameters, *e.g.* the broadening Δ or the energy ε_m , it is in general difficult to determine them from experiment or *ab-initio* calculations. Fortunately, these are only prefactors which change the absolute height of the transition rates and thus can be easily fit to the experiments.

Table 2: The vibrational energy $\hbar\omega$ determined using the potential energy surfaces calculated within DFT.²² The subscript “1” and “2” indicate switching from STM tip to the surface or the reverse process, respectively.

Tip–surface distance	$\hbar\omega_1$ [meV]	$\hbar\omega_2$ [meV]
7.27 Å	40.68	18.95
7.30 Å	40.71	19.00
7.34 Å	40.76	19.06
7.37 Å	40.78	19.12
7.40 Å	40.82	19.15
7.44 Å	40.86	19.22
7.47 Å	40.89	19.26
7.51 Å	40.94	19.32
7.54 Å	40.98	19.37
7.57 Å	41.00	19.42

Table 3: Model-parameters for the switching of the PTCDA between the tip to the surface obtained by fitting R to the experiments. The subscript “1” and “2” indicate switching from STM tip to the surface or the reverse process, respectively. Parameters $\gamma_{eh,1}^{s/t}$ and $\gamma_{eh,2}^{s/t}$ are given in units of $[10^7 \text{ 1/s}]$ or $[10^5 \text{ 1/s}]$, respectively. Energies ϵ_m are given in meV .

Tip–surface distance	$\gamma_{eh,1}^s$	$\gamma_{eh,1}^f$	$\epsilon_{m,1}$	n_1
7.27 Å	8.32	0.98	−979	16
7.30 Å	8.30	0.95	−960	15
7.34 Å	16.03	1.85	−918	15
7.37 Å	12.45	1.36	−831	14
7.40 Å	9.96	1.39	−778	14
7.44 Å	18.11	2.64	−648	14
7.47 Å	7.73	2.13	−528	14
7.51 Å	9.85	3.20	−427	14
7.54 Å	37.47	9.64	−384	14
7.57 Å	30.73	8.25	−346	13

Tip–surface distance	$\gamma_{eh,2}^s$	$\gamma_{eh,2}^f$	$\epsilon_{m,2}$	n_2
7.27 Å	57.16	0.86	262	8
7.30 Å	22.84	5.02	249	9
7.34 Å	5.93	1.70	251	9
7.37 Å	5.30	2.65	242	9
7.40 Å	1.41	0.70	296	10
7.44 Å	0.93	0.46	290	10
7.47 Å	1.72	0.06	271	10
7.51 Å	0.45	0.01	296	10
7.54 Å	0.06	0.01	264	10
7.57 Å	0.01	0.002	283	11

This material is available free of charge via the Internet at <http://pubs.acs.org/>.

References

- (1) G. Binnig, H. Rohrer, Ch. Gerber and E. Weibel, Phys. Rev. Lett. **49**, 57 (1982).
- (2) F. Moresco, Phys. Rep. **399**, 175 (2004).
- (3) D. Eigler and E. Schweizer, Nature **344**, 524 (1991).
- (4) J. A. Stroscio and R. J. Celotta, Science **306**, 242 (2004).

- (5) A. J. Heinrich, C. P. Lutz, J. A. Gupta, and D. M. Eigler, *Science* **298**, 1381 (2002).
- (6) F. Moresco, G. Meyer, K.-H. Rieder, H. Tang, A. Gourdon, and C. Joachim, *Phys. Rev. Lett.* **86**, 672 (2001).
- (7) V. Iancu and S.-W. Hla, *Proc. Natl. Acad. Sci.* **103**, 13718 (2006).
- (8) P. Liljeroth, J. Repp, and G. Meyer, *Science* **317**, 1203 (2007).
- (9) Y. Wang, J. Kröger, R. Berndt, and W. Hofer, *J. Am. Chem. Soc.* **131**, 3639 (2009).
- (10) S. G. Tikhodeev and H. Ueba, *Phys. Rev. B* **70**, 125414 (2004).
- (11) H. Ueba, T. Mii, N. Lorente, and B. N. J. Persson, *J. Chem. Phys.* **123**, 084707 (2005).
- (12) S. G. Tikhodeev and H. Ueba, *Phys. Rev. Lett.* **102**, 246101 (2009).
- (13) M. Cizek, M. Thoss, and W. Domcke, *Phys. Rev. B* **70**, 125406 (2004).
- (14) S. Gao, M. Persson, and B. Lundqvist, *Phys. Rev. B* **55**, 4825 (1997).
- (15) F. Elste, G. Weick, C. Timm, and F. von Oppen, *Appl. Phys. Mater. Sci. Process.* **93**, (2008).
- (16) L.J. Lauhon and W. Ho, *Phys. Rev. Lett.* **85**, 4566 (2000).
- (17) K. Glöckler, C. Seidel, A. Soukopp, M. Sokolowski, E. Umbach, M. Böhringer, R. Berndt, and W. D. Schneider, *Surface Science* **405**, 1 (1998).
- (18) F. S. Tautz, *Prog. Surf. Sci.* **82**, 479 (2007).
- (19) M. Rohlfing, R. Temirov, and F. S. Tautz, *Phys. Rev. B* **76**, 115421 (2007).
- (20) F. Pump, R. Temirov, O. Neucheva, S. Soubatch, S. Tautz, M. Rohlfing, and G. Cuniberti, *Appl. Phys. A* **93**, 335 (2008).
- (21) R. Temirov, A. Lassise, F. Anders, and F. S. Tautz, *Nanotechnology* **19**, 065401 (2008).

- (22) C. Toher and *et al.*, in preparation (2009).
- (23) A. Hauschild, K. Karki, B. Cowie, M. Rohlfiing, F. Tautz, and M. Sokolowski, *Phys. Rev. Lett.* **94**, 036106 (2005).
- (24) A. Y. Kobitski, R. Scholz, and D. R. T. Zahn, *J. Mol. Struct.: THEOCHEM* **625**, 39 (2003).
- (25) D.R. Lide, *CRC Handbook of Chemistry and Physics*. 89 ed. (2008).
- (26) S. Duhm, A. Gerlach, I. Salzmann, B. Bröker, R.L. Johnson, F. Schreiber and N. Koch, *Org. Electron.*, **9**, 111 (2008).
- (27) A.R. Rocha, V.M. García-Suárez, S. Bailey, C. Lambert, J. Ferrer and S. Sanvito, *Phys. Rev. B* **73**, 085414 (2006).